Development 125, 1149-1159 (1998)
Printed in Great Britain © The Company of Biologists Limited 1998
DEV5177

strabismus, a novel gene that regulates tissue polarity and cell fate decisions in *Drosophila*

Tanya Wolff and Gerald M. Rubin*

Howard Hughes Medical Institute and Department of Molecular and Cell Biology, University of California, Berkeley, CA 94720-3200, USA
*Author for correspondence (e-mail:gerry@fruitfly.berkeley.edu)

Accepted 30 December 1997: published on WWW 17 February 1998

SUMMARY

Polarity in the *Drosophila* eye is manifested as a dorsoventral reflection of two chiral forms of the individual unit eyes, or ommatidia. These forms fall on opposite sides of a dorsoventral midline of mirror symmetry known as the equator. Polarity is established in the eye imaginal disc as cells adopt their fates and as the ommatidial precursors undergo coordinated rotation within the epithelium; the mechanisms that coordinate these early patterning events remain poorly understood. We have identified a novel gene, *strabismus* (*stbm*), which is required to establish polarity in the eye, legs and bristles of *Drosophila*. Many *stbm* ommatidia are reversed anteroposteriorly and/or dorsoventrally. In *stbm* eye discs, ommatidial rotation is delayed and some ommatidial precursors initiate rotation in the wrong direction. Mosaic analysis indicates that *stbm* is ommatidium autonomous and required in most, if not all, photoreceptors within an ommatidium to establish normal polarity. *stbm* also appears to play an instructive role during the establishment of the fates of photoreceptors R3 and R4. *stbm* encodes a novel protein with a potential PDZ domain-binding motif and two possible transmembrane domains. Sequence analysis of both vertebrate and invertebrate homologs indicates that *stbm* has been highly conserved throughout evolution.

Key words: *strabismus*, Tissue polarity, Cell fate, *Drosophila*, Eye

INTRODUCTION

The establishment of polarity occurs throughout the development of unicellular and multicellular organisms, both prokaryotic and eukaryotic, and is fundamental for the generation of cellular diversity and tissue specialization. In single cells, the asymmetric distribution of regulatory molecules is required to establish distinct fates in daughter cells (Rhyu et al., 1994; Kraut et al., 1996) and underlies the establishment of specialized anterior and posterior structures, such as dendrites and axons in a neuron, and the specialized apical and basal domains in many cell types. In animal tissues, the polarity of groups of cells is coordinately regulated. This tissue polarity, or polarity within the plane of an epithelium, organizes epithelia into functional units. We are using the developing *Drosophila* eye, a polarized epithelium, as a system to understand the molecular mechanisms governing the establishment of developmental symmetries. We have identified a novel gene, *strabismus* (*stbm*), which plays a critical role in setting up polarity in multiple tissues in the fly.

Polarity is manifested in various ways, depending upon the tissue in which it is expressed. Many epithelia are covered in a coat of bristles and hairs, and these elaborated structures are uniformly oriented in space. In addition, appendages elaborate unique distal and proximal surfaces. In the *Drosophila* eye, the dorsal and ventral halves of the eye are mirror image reflections of one another.

The *Drosophila* compound eye comprises approximately 800 hexagonal unit eyes, or ommatidia, packed in a smooth array. Each ommatidium is a precise assembly of 20 cells: a central core of 8 photoreceptor cells (R1-R8) and 12 non-neuronal support cells. The rhabdomeres, or light-sensitive organelles of the photoreceptors, are arranged in a characteristic asymmetric trapezoid and are identified by their positions within the trapezoid; R3's rhabdomere occupies the point of the trapezoid (Figs 1C, 2C, and Dietrich, 1909). Each eye contains two chiral forms (i.e. mirror image reflections) of the trapezoid which fall on opposite sides of a midline of mirror symmetry known as the equator (Figs 1C, 2E).

Assembly of cells into ommatidial precursors, or preclusters, begins in the eye imaginal disc, the primordium of the adult eye. Recruitment of cells begins posterior to the morphogenetic furrow, a dynamic front of differentiation which progresses from posterior to anterior across the epithelium. Photoreceptor recruitment follows a characteristic sequence, starting with R8 and followed by the pairwise addition of R2/5, R3/4, R1/6 and finally by R7. The remaining cell types are recruited between late larval and mid-pupal development (for review see Wolff and Ready, 1993).

The group of 8 photoreceptor cells is initially bilaterally symmetrical across the anterior-posterior (A/P) axis. As development proceeds, morphological movements break the symmetry so that the ommatidium becomes polarized across

this axis. These morphological movements are associated with the specification of distinct fates in two of the photoreceptor cells: R3 and R4. Within each R3/R4 pair, the cell that is located closest to the midline of the eye disc, the equatorial cell, adopts the R3 fate, and the more lateral cell, the polar cell, adopts the R4 fate (Fig. 1A). Evidence that the R3 and R4 cells differ first becomes apparent in the third instar eye disc when the bilateral symmetry of the photoreceptor precluster breaks down: R4 loses contact with R8 and its cell body becomes displaced relative to that of R3 (Fig. 1B; and Tomlinson, 1985). The chirality of an ommatidium is therefore associated with the adoption of the R3 and R4 fates.

Two events contribute to the origin of the equator in the third instar eye disc. First, chiral forms are created as a consequence of R3 and R4 adopting their appropriate fates with respect to their dorsal or ventral location in the eye (Fig. 1B). Second, the ommatidial precursors in the dorsal and ventral halves of the eye rotate as units, 90° in opposite directions to one another (Fig. 1A,B; and Ready et al., 1976). As a result of these patterning events, the adult eye displays global mirror symmetry (Figs 1C, 2C,E).

A number of genes are involved in setting up this polarity. *frizzled* (*fz*) encodes a protein with 7 transmembrane domains and is a member of the serpentine class of receptors (Vinson et al., 1989). *fz* ommatidia display an assortment of disruptions in ommatidial polarity, including partial rotations, reversals on either their A/P, dorsal/ventral (D/V) or both A/P and D/V axes (Zheng et al., 1995). *dishevelled* (*dsh*) mutant eyes resemble *fz* eyes (Theisen et al., 1994). Dsh contains a PDZ domain (Klingensmith et al., 1994; Theisen et al., 1994), suggesting it may be localized at sites of cell-cell contact (for review see Fanning and Anderson, 1996). The *Drosophila* homolog of the p21 GTPase RhoA has recently been shown to be required for the generation of tissue polarity. The *RhoA* eye phenotype is similar to that of *fz* and *dsh* and genetic interactions suggest RhoA is a component of the signaling pathway mediated by Fz and Dsh (Strutt et al., 1997). In addition to their eye phenotypes, *fz*, *dsh* and *RhoA* mutant flies also show a variety of polarity defects in other epithelia and cell types. Finally, there are eye-specific genes, such as *nemo* and *roulette*, which carry out the rotation program (Choi and Benzer, 1994).

We have identified a novel gene, *strabismus* (*stbm*), which affects the planar polarity of multiple structures in *Drosophila*. *stbm* ommatidia display anteroposterior, dorsoventral and both anteroposterior and dorsoventral reversals. Our results suggest these phenotypes are likely to be caused by a defect in specification of the R4 cell fate. Mosaic analysis indicates that *stbm* is ommatidium-autonomous and is required in most, if not all, photoreceptor cells for normal orientation. The *stbm* locus encodes a novel protein that has been highly conserved through evolution and contains two putative transmembrane domains as well as a potential PDZ domain-binding motif.

MATERIALS AND METHODS

Genetics

Fly culture and crosses were carried out according to standard procedures. X-irradiation (4000 rads) was used as the mutagen in the FLP/FRT screening strategy (Xu and Rubin, 1993) to identify genes that play a role in eye development. A total of 104,000 flies were screened and 39 mutants required for eye development were identified. Of these, 12 were mutations in the *stbm* locus, and both genetically null and hypomorphic alleles were isolated. 11 additional alleles, also X-irradiation-induced, were identified in a complementation screen. The FLP/FRT system was used to generate clones for mosaic analysis in alleles $stbm^{6cn}$, $stbm^{15cn}$ and $stbm^{10cn}$. Phenotypic analysis was performed on $stbm^{6cn}$, a molecular null allele. Standard genetic crosses were conducted to generate H123; *stbm* and double mutant stocks. Alleles used for genetic interaction studies include fz^{1}, dsh^{1}, nmo^{P1}, pk^{1} and $sple^{1}$.

Histology

Scanning electron microscopy was performed as described by Kimmel et al. (1990). Fixation and sectioning of adult eyes were

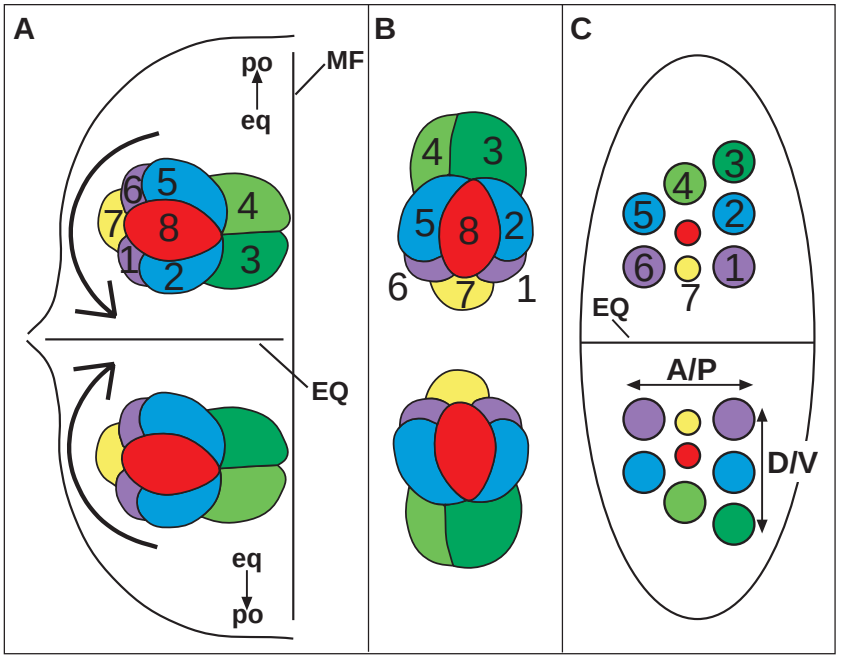

Fig. 1. Origin of the equator in the *Drosophila* eye. Schematic of an eye disc from a third instar larva (A,B) and adult eye (C). The equator originates in the third instar larval eye disc. The photoreceptor precluster is initially symmetrical across its A/P axis. As development proceeds, the preclusters in the dorsal (top) and ventral (bottom) halves of the eye rotate by 90° in opposing directions (arrows) bringing them into the orientation shown in B. The symmetry is broken when R4 loses its contact with R8, as seen in B. In the adult, the rhabdomeres of the photoreceptors are arranged in an asymmetrical trapezoid and are identified based on their position within the trapezoid. Photoreceptors R1, R2 and R3 define the anterior face and R5 and R6 the posterior face of the trapezoid. R3 and R4 lie on the ommatidium's polar face and R1, R7 and R6 lie along the equatorial face. The 'point' of the trapezoid is occupied by R3. The trapezoid comes in two chiral forms which fall on opposite sides of the equator. MF, morphogenetic furrow; EQ, equator; eq, equatorial; po, polar; D/V, dorsoventral axis; A/P, anterior-posterior axis. Anterior is to the right in all figures.

performed as described by Tomlinson and Ready (1987). Lead sulfide staining was performed according to Wolff and Ready, (1991) and cobalt sulfide staining according to Melamed and Trujillo-Cenoz (1975). Elav and lead sulfide staining and mitotic labeling (bromodeoxyuridine (BrdU)-pulsed eye discs) were used to demonstrate that the center-lateral growth of rows is normal in *stbm* eyes. BrdU labeling was performed as described by Wolff and Ready (1991), except that pepsin digestion was omitted. Antibody and X-gal staining were performed according to standard methods. The full length *stbm* cDNA was used as a template to generate the RNA probes used for tissue in situ hybridizations, which were performed as described by Dougan and DiNardo (1992).

Isolation of genomic DNA and cDNA

A P1 phage insert (Berkeley *Drosophila* Genome Project clone DS00300) was used to probe genomic blots of X-ray-induced *stbm* alleles according to standard procedures (Sambrook et al., 1989). A polymorphic 10 kb *Eco*RI fragment was identified in $stbm^{10cn}$ and was used to screen both a *Drosophila* eye-antennal imaginal disc library (prepared by A. Cowman) and a cosmid library of *D. melanogaster* genomic DNA (Tamkun et al., 1992). A human EST (I.M.A.G.E. Consortium (LLNL) cDNA Clone ID no. 120749; Accession no. T95333; Lennon et al., 1995) was used as a probe to screen a mouse PCC4 teratocarcinoma cDNA library (Stratagene). Transformation rescue experiments were conducted using the pGMR expression vector (Hay et al., 1994) containing the 2.1 kb *Eco*RI fragment of the *stbm* cDNA.

DNA sequencing

DNA sequence was determined using the dideoxy chain termination procedure (Sanger et al., 1977) using Automated Laser Fluorescence (Pharmacia) and Applied Biosystem, Inc. 373 sequencers. Templates were prepared by sonication and insertion of plasmid DNA into the M13mp10 vector. The entire coding regions as well as the genomic regions that correspond to the *stbm* locus were sequenced on both strands. Sequences were analyzed using the Staden (R. Staden, Medical Research Council of Molecular Biology, Cambridge, England) and the Genetics Computer Group, Inc. software packages. Genomic libraries of X-ray-induced and cytologically normal *stbm* alleles were constructed using the lambda ZAP expression vector (Stratagene).

RESULTS

Identification of *stbm*

stbm was identified by virtue of its rough eye phenotype in mosaic clones in the *Drosophila* eye. The FLP/FRT system was used to generate clones of X-irradiation-induced mutant tissue in a heterozygous background (Golic and Lindquist, 1989; Xu and Rubin, 1993). Externally, mutations in the *stbm* locus are manifested as a mild roughening of the normally smooth ommatidial lattice (Fig. 2B). *stbm* is a recessive, homozygous viable mutation, although null alleles display reduced viability.

Ommatidial polarity is disrupted in *stbm* mutant eyes

In *stbm* mutant eyes the normally parallel rows of ommatidia are not properly aligned, giving the eyes a rough appearance (Fig. 2B; compare to wild type, 2A). Tangential sections through adult eyes indicate that the vast majority of *stbm* ommatidia are correctly assembled (Fig. 2D; compare to wild type, 2C) and that the misaligned eye lattice is a consequence of aberrant orientation of ommatidial units. *stbm* ommatidia show several orientations: they are either normal, reversed dorsoventrally, anteroposteriorly, or both dorsoventrally and anteroposteriorly. In addition, while most ommatidia rotate the normal 90°, many undergo either partial or no rotation. Finally,

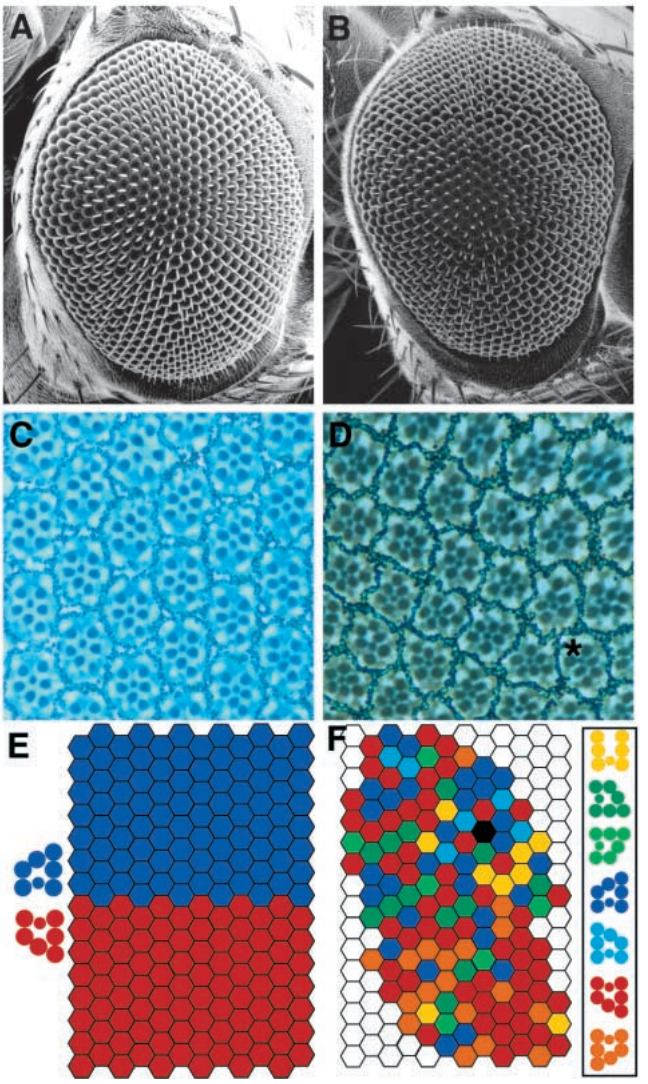

Fig. 2. Ommatidial polarity is disrupted in *stbm* eyes. SEMs of wild-type (A) and *stbm* (B) adult eyes. Misorientation of ommatidia in *stbm* homozygous eyes disrupts the normally smooth lattice of ommatidia, giving the eye a 'rough' appearance. Tangential sections through wild-type (C) and *stbm* (D) adult eyes and schematic representations of the sections (E and F). The two normal chiral forms of trapezoids are shown in red and dark blue. The equator is abolished in *stbm* eyes because mutant ommatidia come in a variety of orientations (D, F and key). *stbm* ommatidia show inversions on their A/P, D/V, and both axes and many ommatidia do not rotate a full 90°. Some ommatidia completely fail to rotate. For simplicity, the degree of rotation of each of the ommatidia is not depicted in the schematic; ommatidia that were not oriented perpendicular to the equator were assigned to the color code that most closely approximated their angle of orientation. Key: dark blue, normal dorsal eye; red, normal ventral eye; light blue, A/P inversion of dorsal eye; orange, A/P inversion of ventral eye; light and dark green, unrotated (both chiral forms); yellow, 'rectangular trapezoids' (Fig. 2D-asterisk). One ommatidium was missing a single photoreceptor and is indicated in black.

in a small percentage of ommatidia, photoreceptors R3 and R4 are bilaterally symmetrical so the chirality of the ommatidium is abolished. The arrangement of rhabdomeres in these achiral ommatidia is rectangular rather than trapezoidal (Fig. 2D-asterisk, F-yellow). We have named this gene *strabismus*, which is formally defined as "a disorder of vision due to a deviation from normal orientation of one or both eyes" and is the medical term for 'cross-eyed'.

To determine the relative proportions of the various ommatidial forms, polarity of genetically mutant ommatidia was quantitated in clones of homozygous *stbm*^{6cn} tissue, a molecular null allele. The equator in the surrounding wild-type tissue provided a reference for a mutant ommatidium's dorsal vs. ventral position in the eye. Of 181 ommatidia scored, 46% showed normal orientation, 35% showed D/V pattern reversals, 7% displayed A/P reversals, 7% were reversed both dorsoventrally and anteroposteriorly, 3% failed to rotate and 2% were achiral.

As a consequence of ommatidial misorientation, the pigment cell lattice is disrupted. Cobalt sulfide-stained pupal eyes reveal that *stbm* eyes contain a normal complement of primary pigment cells, bristles and cone cells, although occasional ommatidia are missing one cone cell. Secondary and tertiary pigment cell numbers are often correct, except at the vertices of partially or unrotated ommatidia where there is an excess of these cell types (data not shown).

Ommatidial rotation is delayed in *stbm* eye discs

To assess ommatidial rotation, eye discs were stained with an antibody that recognizes the nuclear neuron-specific protein Elav (Fig. 3A,B) (Robinow and White, 1991), or cobalt and lead sulfide, which highlight the apical surfaces of cells (Fig. 3C,D). The Elav-stained discs demonstrate that *stbm* does not play a role in recruiting photoreceptors into the assembling ommatidium, as photoreceptors are recruited in the normal sequence and with normal timing in mutant discs (Fig. 3B, compare to wild type, Fig. 3A).

Views of the apical surface of eye discs indicate that ommatidial rotation normally begins approximately 5 rows posterior to the furrow and is complete by row 12 (Fig. 3A,C). In *stbm* eye discs, the majority of preclusters are delayed in initiating rotation (Figs 3B,D – asterisks and 4F). As the photoreceptor preclusters mature, their tips become effaced from the apical surface of the disc so their orientation can no longer be evaluated at the apical surface. However, the cone cells, which lie on top of the photoreceptor cells in stereotypic positions, provide a useful compass by which to measure ommatidial orientation at the posterior of the third instar eye disc. Observations of cone cells in lead and cobalt sulfide-stained mutant eye discs reveal that the majority of ommatidial preclusters at the posterior of *stbm* eye discs have rotated no more than approximately 45° whereas wild-type precursors would have rotated 90° at an equivalent point in development (not shown). Of those ommatidia that do begin to rotate on schedule, most appear to initiate rotation in the correct

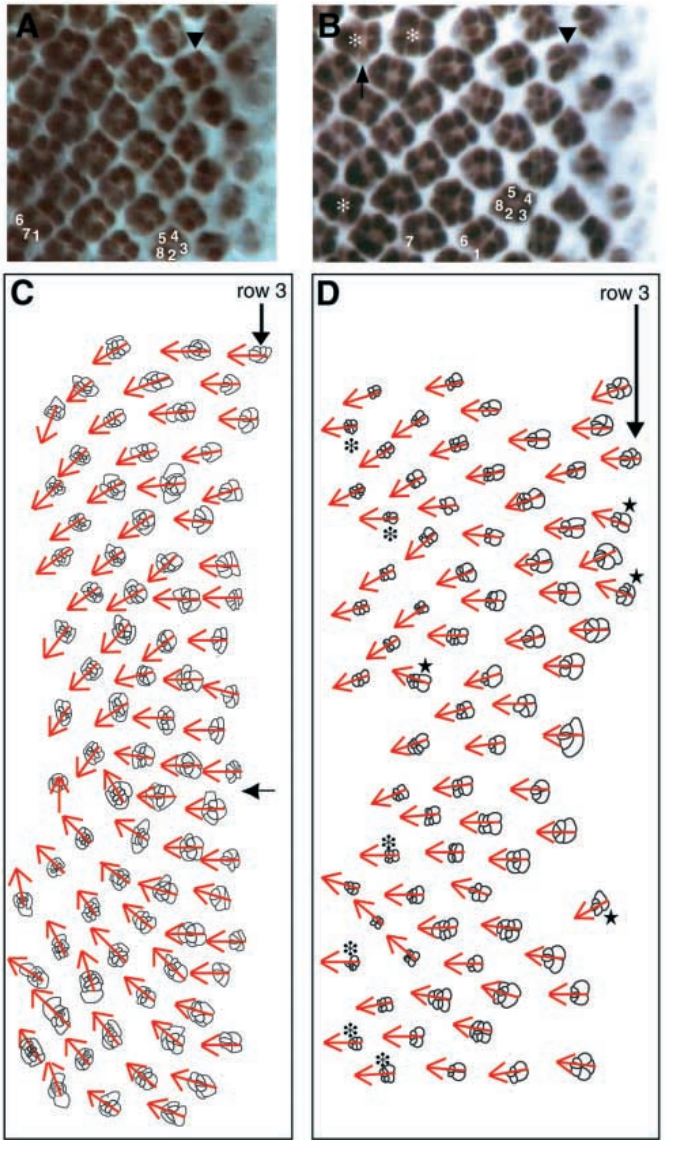

Fig. 3. Ommatidial assembly is normal but rotation is delayed in *stbm* eye discs. Elav-stained third instar eye imaginal discs from wild-type (A) and *stbm* (B) larvae. Recruitment of photoreceptors in *stbm* mutant eyes follows the normal 8, 2/5, 3/4, 1/6, 7 sequence and the arrangement of photoreceptors is normal (B). In wild-type eye discs, rotation first becomes evident in the fifth Elav-stained row (arrowhead). In mutant eye discs, photoreceptor preclusters in the fifth stained row (arrowhead) typically have not yet begun to rotate, and even by the 12th row (arrow), many ommatidia do not show signs of rotation. Several preclusters that have not initiated rotation by rows 9-12 are indicated by asterisks. Video lucida drawings of wild-type (C) and *stbm* (D) third instar eye imaginal discs. Regions shown here span the central region of the eye disc. Ommatidial precursors are overlaid with vectors indicating the degree of ommatidial orientation. In wild-type eye discs the vectors in the dorsal half of this right eye rotate counterclockwise and those in the ventral half rotate clockwise in a graded fashion from anterior to posterior across the eye disc. By approximately row 12, ommatidial precursors have completed their rotation and the vectors lie perpendicular to the equator (beyond the limit of the image shown here). The equator is marked with an arrow. In *stbm* eye discs, the equator does not exist because the vectors do not converge on a single interface (D), but since this tracing was taken from the center of the disc, the midline coincides with the arrow in C. In *stbm*, some preclusters do begin to rotate on time, but the majority show a delay in rotation; as late as rows 10-12, many ommatidia show only slight or no change in orientation (asterisks). Of those preclusters that do rotate, some rotate in the wrong direction (stars). Dorsal is up.

direction with respect to their dorsal or ventral location within the epithelium, but some initiate rotation in the wrong direction (Fig. 3B).

These preparations demonstrate that ommatidial orientation is disrupted in two ways during the initial stages of pattern formation. First, ommatidial rotation is significantly delayed in *stbm* eye discs and second, some ommatidial precursors initiate rotation in the wrong direction.

Equator-lateral growth of a row is not disrupted in *stbm* eye discs

The position of the future equator is evident in the third instar eye disc prior to the start of ommatidial rotation. New rows emerging from the furrow are initiated at the D/V midline (the site of the future equator) and grow laterally as ommatidia are added to each end in a symmetrical manner (Wolff and Ready, 1991). This 'center-lateral' growth of a row and ommatidial rotation are both affected in *fz* mutants (Zheng et al., 1995), suggesting these two events may be linked. However, while the adult phenotypes of *fz* and *stbm* are similar, the center-lateral growth of a row is not altered in *stbm* mutants (see Methods, data not shown). This observation indicates that the two events are genetically separable and that *stbm* may act downstream of *fz*, or in a parallel pathway, in its role in orientation but not in its role in the center-lateral growth of new ommatidial rows.

The R3 and R4 fates are mis-specified in *stbm*

The aberrant ommatidial forms seen in *stbm* mutant eyes (Fig. 2F) can be accounted for by invoking defects in either chirality, rotational direction or both (Fig. 4A,B; see legend for details). To distinguish between these possibilities we used the enhancer trap line H123, which is differentially expressed in R3 and R4 and therefore provides a molecular marker to differentiate between these two cell fates (Fig. 4C,E). We examined H123 expression in a null *stbm* allele and found both reversals in specification of the R3 and R4 cell fates and misrotations (Fig. 4D,F ; see legend for details). Four classes of preclusters were seen in *stbm* discs and these correlate with the predicted classes described in Fig. 4A. Ommatidia were seen in which the R3 and R4 fates were correctly specified and rotation occurred in either the correct (Fig. 4D,F: no. 1) or incorrect (no. 4) direction with respect to the R3 and R4 fates. In addition, ommatidia were seen in which the R3 and R4 fates were

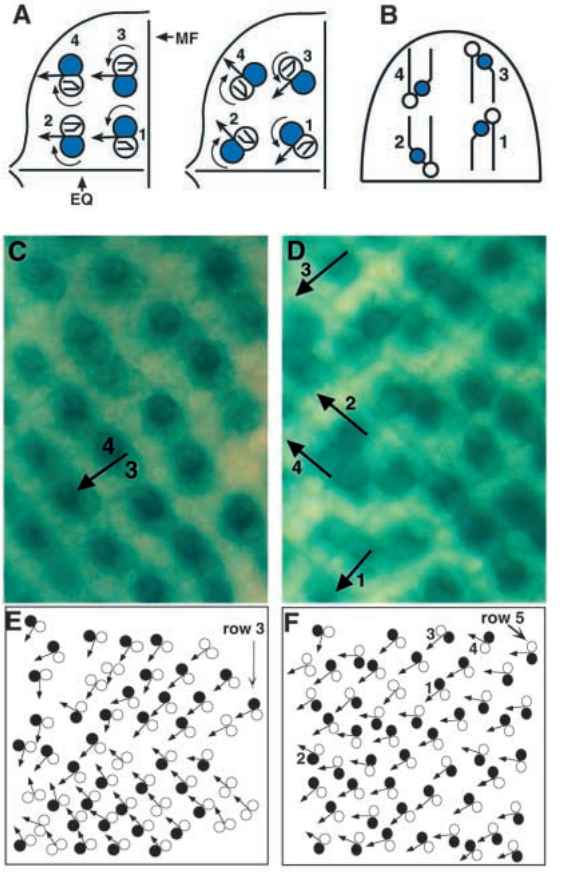

Fig. 4. Photoreceptor fates R3 and R4 are mis-specified in *stbm* eye discs. (A) Schematic illustrating the origin of the various mis-oriented ommatidia seen in adult eyes. Only the dorsal half of the eye disc is shown. The two cells shown here are R4, the filled circle, and R3, the circle containing the trapezoid. As in Fig. 3, the vector between R3 and R4 indicates the direction of orientation of the preclusters; prior to the initiation of rotation, all vectors were oriented perpendicular to the MF. The curved arrows indicate the direction in which the preclusters are turning. The trapezoids embedded in the R3 cells indicate the projected adult form for each example illustrated. These adult forms are shown at the completion of their 90° rotation in the adult eye in B. No. 1 represents a normal precluster in which the polar cell is R4 (H123 positive) and the precluster is rotating correctly. No. 2 represents a precluster in which the wrong cell of the R3/R4 pair, the equatorial cell, adopted the R4 fate; this cluster is rotating correctly with respect to the cell that adopted the R4 fate. This cluster will give rise to an adult ommatidium that is dorsoventrally inverted. No. 3 illustrates a cluster in which the equatorial cell adopted the R4 fate and the precluster is rotating incorrectly relative to the cell that adopted the R4 fate. This class of preclusters will give rise to ommatidia that are anteroposteriorly inverted. No. 4 is an example of a precluster in which the polar cell adopted the R4 fate, but the ommatidium is misrotating so that the adult form will be inverted both anteroposteriorly and dorsoventrally. (B) The trapezoids shown in A have not yet completed their full 90° of rotation. They are illustrated at the completion of this event, in their adult orientation, in B. (C,D) The dorsal regions of H123 enhancer trap eye discs from wild-type (H123/+ ; C) and *stbm* (*stbm* ^{6cn}/*stbm* ^{6cn}; H123/+ ; D) larvae stained for β-galactosidase activity. In H123 discs, β-gal is expressed in both R3 and R4, but expression levels are higher in R4, the polar cell. The arrows indicate the orientation of the clusters and are drawn between R3 and R4. The 4 aberrant forms of preclusters outlined in A were seen in mutant eye discs. One example of each type is indicated in D and F; numbering is as in A. In C and D, the equator is below the panel's border. Schematic of wild-type (E) and *stbm* (F) eye discs in an H123 background. Drawings span the central region of the eye discs. Filled circles indicate H123-positive R4 cells and unfilled circles represent R3 cells. Occasionally, the intensity of staining between R3 and R4 was equivalent; in these cases, both circles were left unfilled. The vectors indicate the orientation of the preclusters and converge on the midline in wild type. In *stbm*, fate mis-specifications and misrotations are evident (D,F). Normal preclusters were seen in which the polar cell of correctly rotating groups was more intensely stained (A,D,F, no. 1). In some clusters the equatorial cell of the R3/R4 pair was more strongly stained and rotation occurred in the direction appropriate for the given R3/R4 fates (A,D,F, no. 2). Two groups of clusters misrotated with respect to the cell that adopted the R4 fates: clusters in which the equatorial cell adopted the R4 fate (A,D,F, no. 3), and clusters in which the polar cell adopted the R4 fate (A,D,F, no. 4). The delay in rotation in *stbm* is also evident in F.

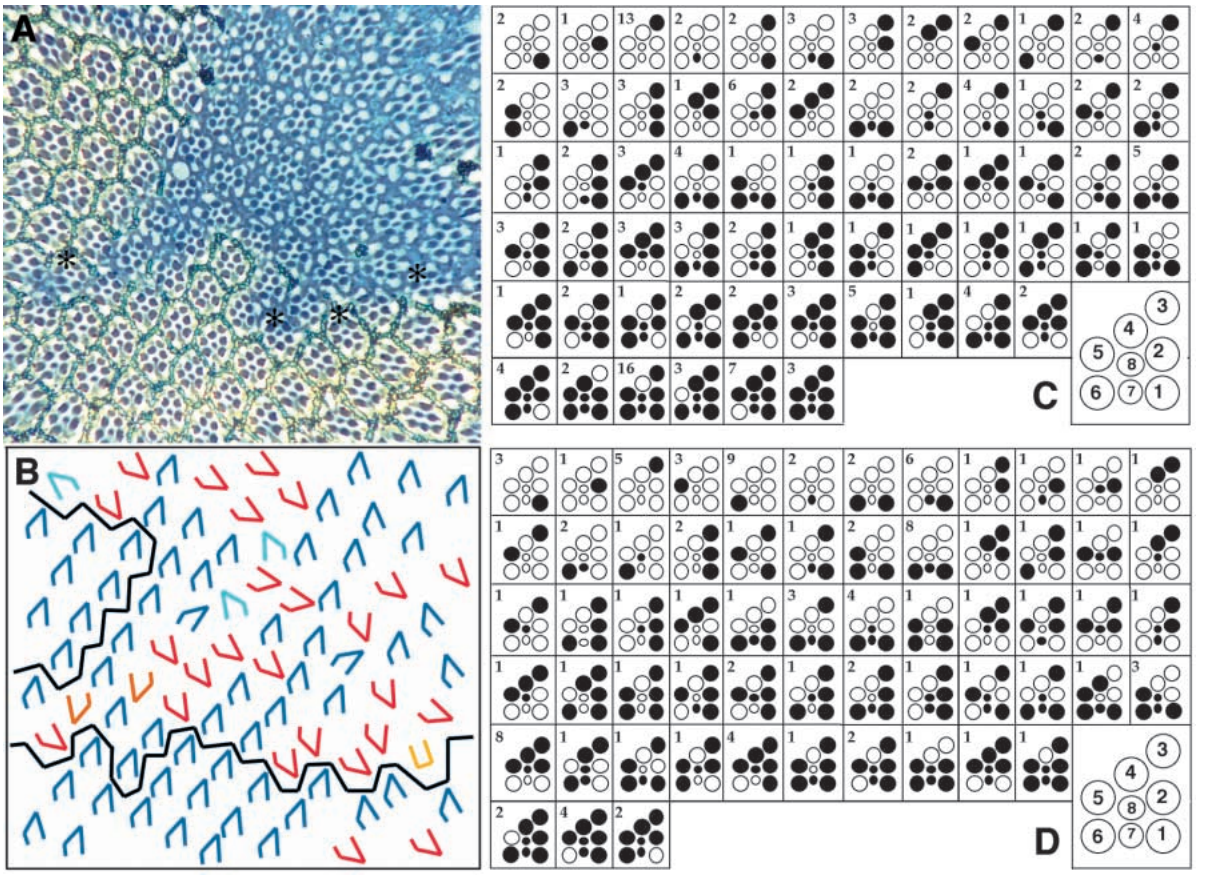

Fig. 5. *stbm* acts autonomously within an ommatidium to direct ommatidial orientation. (A) Section through a *stbm* clone. The *stbm* ^{10}/*stbm* ^{10} clone is marked by the absence of pigment granules whereas wild-type tissue is marked by the presence of pigment granules. Within the clone, ommatidia show misrotations and misorientations typical of those seen in homozygous eyes. Along the clonal border, ommatidia can be misoriented (asterisks). The equator is seen in the wild-type tissue in the lower portion of the panel (see B). (B) A schematic of the trapezoids corresponding to the clone in A. The black lines delineate genotypically wild type from mutant ommatidia; mosaic ommatidia are included in the mutant region. Genetically wild-type ommatidia do not show errors in orientation (trapezoids outside the clonal region are all blue above the equator and red below the equator, indicating normal orientation). Trapezoids are color coded according to the scheme shown in Fig. 2F and therefore indicate an ommatidium's phenotype. (C and D) Summary of mosaic analysis for phenotypically mutant (misoriented; C) and phenotypically wild-type (D) ommatidia. Genetically mutant photoreceptors are illustrated as filled circles and genetically wild-type photoreceptors by open circles. Numbers in the upper left hand corners of each box indicate the number of examples of each combination of photoreceptors that were observed. Key in lower right identifies each photoreceptor by number according to its position within the trapezoid. We have not seen misoriented mosaic ommatidia in which each R alone is mutant and therefore cannot conclude that each photoreceptor is required for normal orientation. It is likely that the low frequency of ommatidia in which only one photoreceptor cell was mutant precluded the identification of all possible mutant:wild-type photoreceptor combinations.

reversed and rotation occurred in either the correct (no. 2) or incorrect (no. 3) direction with respect to the R3 and R4 fates. This analysis of H123 expression in *stbm* discs suggests that *stbm* may participate in imparting the R3 and R4 fates and it therefore follows that the phenotype results from a failure in fate specification rather than later patterning events involving placement of the R3 and R4 rhabdomeres.

We have also examined lead sulfide-stained *stbm* eye discs to assess cell contacts within the photoreceptor preclusters. In wild-type eye discs, the symmetry in the 8 cell precluster is lost when R4, the polar cell of the R3/R4 pair, loses contact with the central photoreceptor, R8 (Fig. 1B). In some preclusters in *stbm* eye discs the equatorial cell loses contact with R8 (data not shown). These findings are consistent with the H123 results described above and suggest that *stbm* participates in the specification of the R3 and/or R4 fates.

The fact that the R3 and R4 fates can be mis-specified in *stbm* ommatidia raises the possibility that the fates of the remaining symmetrical photoreceptor pairs, R2/R5 and R1/R6, are also reversed, such that the anterior and posterior faces of the trapezoid are inverted. Because molecular markers that distinguish between the members of these photoreceptor pairs do not exist, it is not possible to address this question directly. However, in wild-type ommatidia, R8's rhabdomere extends between R1 and R2 (Dietrich, 1909), and only rarely between R5 and R6 (R. Cagan, personal communication), suggesting R8 can recognize a difference between cells to the anterior, R1 and R2, and those to the posterior, R5 and R6. If we assign the R3 fate to the cell occupying the point of the trapezoid, then in *stbm* ommatidia, R8 extended its rhabdomere between R1 and R2 in 95 out of 96 cases examined. These results are consistent with the notion that the anterior (R1, R2 and R3)

and posterior (R4, R5, and R6) cell fates may be switched in *stbm* ommatidia, and that the entire ommatidium is 'backwards'.

stbm is ommatidium autonomous and is required to specify the R4 cell fate

stbm could be directing ommatidial orientation by one of several mechanisms. It could act locally to coordinate the process within an ommatidium or between neighboring ommatidia, or it could provide a diffusible polarity signal across the entire disc. To distinguish between these possibilities, we analyzed ommatidia located in and near clones of homozygous mutant *stbm* tissue. First, we found that clones anywhere in the disc are autonomous. Consistent with this observation, we have found *stbm* RNA throughout the eye disc using *stbm* as a probe for in situ analysis (not shown).

Second, we assessed the phenotype of genotypically mutant ommatidia lying along the border of the clone. We found that genotypically mutant (as well as mosaic) ommatidia are not rescued by their wild-type neighbors (Fig. 5A, asterisks) – they misrotate even when located next to genotypically wild-type ommatidia. Third, genetically wild-type ommatidia are not affected by neighboring mutant tissue (Fig. 5B, dark blue ommatidia, see legend for details). Therefore, *stbm* acts autonomously within ommatidia; in other words, the presence or lack of Stbm function in one ommatidium does not affect the polarity of neighboring ommatidia.

To establish if *stbm* acts in one specific cell to establish orientation of the entire ommatidium, we carried out a mosaic analysis of ommatidia displaying either mutant (Fig. 5C) or normal (Fig. 5D) orientation. We randomly chose 169 misoriented and 119 normally oriented mosaic ommatidia at clonal boundaries and scored the genotype of photoreceptors within these ommatidia. Our overall observation from both phenotypically mutant and wild-type mosaic ommatidia is that misorientation or normal orientation does not correlate absolutely with the mutant genotype of any specific photoreceptor or group of photoreceptor cells. Specifically, the combination of *stbm* mutant and wild-type photoreceptors does not predict the orientation of the ommatidium. Rather, many of the photoreceptors make a contribution.

However, we have also noticed some interesting biases in the frequency with which certain photoreceptors were mutant. First, there is an over-representation of *stbm*$^-$ R3 cells in misoriented mosaic ommatidia: 87% of misoriented ommatidia have a mutant R3 cell. Second, *stbm*$^-$ R4 cells are under-represented: 26% of misoriented ommatidia and 21% of properly oriented mosaic ommatidia have a mutant R4 cell (Table 1). This suggested two possibilities: (1) *stbm* is required in R3 for proper orientation or (2) *stbm* is required to specify the R4 cell fate. We therefore analyzed mosaic ommatidia in which the R3/R4 pair is mosaic ($R3^+/R4^-$ or $R3^-/R4^+$). We found a total of 144 such cases, 141 of which were of the $R3^-/R4^+$ type. This implies that if one of the R3/R4 pair is mutant it will become an R3. Thus, Stbm is required for the R4 cell to establish its fate.

Furthermore, the choice of the R3/R4 cell fate appears to in turn influence the direction of ommatidial rotation. Consistent with this is the observation that of these 141 $R3^-/R4^+$ ommatidia, 74% acquire an incorrect orientation while only 26% adopt the correct orientation. If both cells are mutant, 59% are incorrectly oriented and 41% are correctly oriented, as would be expected if orientation becomes random. However, while having $R3^+$ and $R4^+$ increases the probability of correct orientation, it is not sufficient as 73% are correctly oriented and 27% are incorrectly oriented. These data are consistent with the results obtained using the H123 marker.

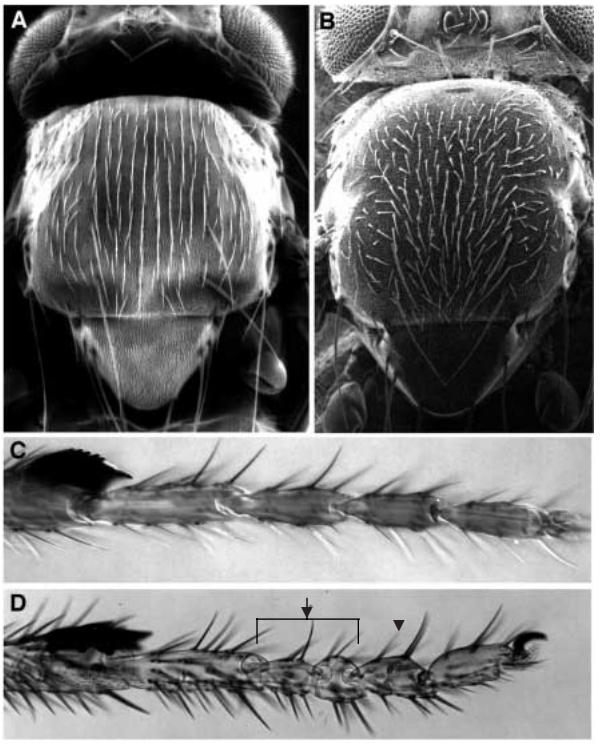

Fig. 6 *stbm* affects the polarity of multiple structures. SEMs of wild-type (A) and *stbm* (B) thoraxes. In wild type, the bristles and hairs are uniformly oriented in space whereas in *stbm* flies, the polarity of these structures is drastically disrupted. Light micrographs of the first leg from a male wild-type (C) and *stbm* (D) fly showing the 5 tarsal segments. In the mutant leg, both a duplication (4th tarsal segment, arrow) and a partial duplication (3rd tarsal segment, arrowhead) are evident.

In summary, two conclusions can be drawn from the mosaic analysis. First, Stbm is ommatidium autonomous and the presence of the normal gene product in any one cell is not sufficient to establish correct orientation; rather, it is required in many, if not all, photoreceptors. This result suggests that each photoreceptor makes some contribution to the orientation process which must be a highly coordinated effort between cells within an ommatidium. Second, Stbm appears to be important in specifying the fate of the R4 cell.

stbm affects the polarity of multiple structures

stbm affects the polarity of multiple tissues in *Drosophila*. In *stbm*, the polarity of many of the bristles and hairs is abnormal. In wild-type animals, the thoracic bristles and hairs are aligned in parallel rows with each bristle pointing toward the posterior of the animal (Fig. 6A) while the leg bristles lie flat against the leg surface and point distally. In *stbm* homozygotes, many thoracic bristles have aberrant polarity (Fig. 6B) and the leg bristles are oriented perpendicular to the leg. Hair polarity is disrupted throughout the body, for example surrounding the

Table 1. Distribution of mutant photoreceptors in misoriented and correctly oriented mosaic ommatidia

strb-photoreceptor	Misoriented ommatidia	Correctly oriented ommatidia
R1	56	48
R2	54	37
R3	87	46
R4	26	21
R5	43	34
R6	42	38
R7	57	39
R8	60	35

eye and on the wings and thorax (not shown). *stbm* also plays a role in setting up the cuticular polarity of the legs. In *stbm* legs, extra tarsal segments or partial duplications (Fig. 6D, arrow and arrowhead, respectively; compare to Fig. 6C) frequently occur in tarsal segments 3 and 4 and occasionally in tarsal segment 2 (see Held et al., 1986 for detailed description of this phenotype). Finally, the wings of *stbm* flies are held out (not shown). This widespread requirement for *stbm* in various tissues is not uncommon among tissue polarity mutants; for example, *fz*, *dsh*, *prickle* (*pk*) and *spiny legs* (*sple*) affect the polarity of various structures, including bristles, hairs and the leg (see Gubb, 1993 for review). These apparently very distinct types of polarity are clearly being regulated by the same basic processes, yet the cellular basis and common theme underlying these various phenotypes remains to be established.

stbm also plays a role in early embryonic development, as many homozygous embryos die between 0-4 hours following egg laying. We have not yet determined the role for *stbm* during these early developmental events.

The *stbm* gene encodes a novel protein with a putative PDZ domain-binding motif

The *stbm* locus was meiotically mapped to 2-61 and cytologically mapped to 45A7-10 based on polytene chromosome analysis of X-ray-induced *stbm* alleles. A P1 phage insert (see Methods) covering this locus was used to screen genomic DNA blots prepared from X-ray-induced *stbm* alleles. A polymorphism was identified in a 10 kb *Eco*RI fragment in allele $stbm^{10cn}$. This genomic fragment was used to screen an eye-antennal imaginal disc cDNA library which identified a single class of cDNAs. The longest cDNA (3.4 kb) was sequenced and found to contain a single ORF, 1.9 kb in length; this ORF predicts a protein of 584 amino acids. Sequence analysis of the corresponding genomic region revealed that the gene contains no introns.

BLAST searches of protein and nucleotide databases indicate that *stbm* encodes a novel protein. Amino acid sequence analysis of the putative Stbm protein reveals 4 hydrophobic stretches in the N-terminal third of the protein, the longest of which spans 29 amino acids, suggesting a possible transmembrane localization for the protein (Fig. 7). The four C-terminal amino acids of the protein, ETSV, are of particular interest as they match a consensus sequence for PDZ domain-binding motifs (X S/T X V; Songyang et al., 1997).

Confirmation that this gene corresponds to the *stbm* locus was provided by sequence analysis of 4 mutant alleles. Alleles $stbm^{6cn}$, $stbm^{153}$ and $stbm^{15cn}$ contain small deletions and $stbm^{60}$ is a duplication of adjacent bases; all four mutations lie within the ORF and cause frame shift mutations in the ORF (Fig. 7). Further confirmation comes from transformation rescue experiments in which the *stbm* cDNA was expressed in cells posterior to the morphogenetic furrow in the eye imaginal disc using a *glass* responsive promoter (Hay et al., 1994). While the eye phenotype was rescued in these flies, other *stbm* phenotypes were not rescued (not shown).

Stbm has been highly conserved through evolution

A search of translated nucleotide databases using the TBLASTN program (Altschul et al., 1990) identified a human EST (I.M.A.G.E. cDNA Clone no. 120749-see Methods) with homology to Stbm. Complete sequence of this partial cDNA revealed that the C-terminal half is 55% identical and 72% similar to the fly homolog (Fig. 7). The human EST was used to screen a mouse teratocarcinoma cDNA library. The longest cDNA identified (3.7 kb) was sequenced; sequence comparison showed that the mouse protein is 50% identical to the fly protein with the C terminus showing a greater degree of conservation. We also identified a *C. elegans* homolog through a search of the *C. elegans* database (Accession no. U52000); the *Drosophila* and *C. elegans* proteins are 33% identical. The four hydrophobic domains and the PDZ domain-binding motif are conserved among the four species (Fig. 7).

DISCUSSION

The mechanisms that regulate the establishment of tissue polarity during development are poorly understood and are likely to vary depending on the epithelial type. We report the role of a novel gene, *stbm*, which is involved in setting up polarity in the *Drosophila* eye. *stbm* plays a role in coordinating the fate specification of photoreceptors R3 and R4 in the dorsal and ventral halves of the eye. The rotation machinery subsequently acts to induce rotation, thereby establishing global mirror symmetry in the eye.

The role of *stbm* in establishing polarity in the retina

Ommatidia in *stbm* mutant eyes display an array of orientation defects, including dorsoventral, anteroposterior, or both dorsoventral and anteroposterior reversals. In addition, many ommatidia fail to complete the full 90° of rotation and some fail to rotate altogether. Finally, in a small proportion of ommatidia, the R3 and R4 rhabdomeres are symmetrically positioned, forming rectangles rather than trapezoids. Defects in both fate specification and ommatidial rotation must be invoked to account for these various ommatidial forms. Our studies implicate *stbm* in playing a primary role in fate specification and possibly a minor role in rotation.

Two lines of evidence illustrate *stbm*'s role in specifying the fate of the R4 cell. First, enhancer trap line H123, which is expressed more intensely in the polar cell than the equatorial cell in wild-type discs, is expressed more intensely in the equatorial than the polar cell in some $stbm^{-}$ preclusters. This result suggests that these fates are often reversed in the mutant. Second, the mosaic analysis indicates *stbm* function is absolutely required to assign the R4 fate: in mosaic ommatidia in which one of the R3/R4 pair is mutant, the $stbm^{+}$ cell becomes an R4 cell in 98% of cases.

While *stbm* is required for the R4 cell identity, the R3 and

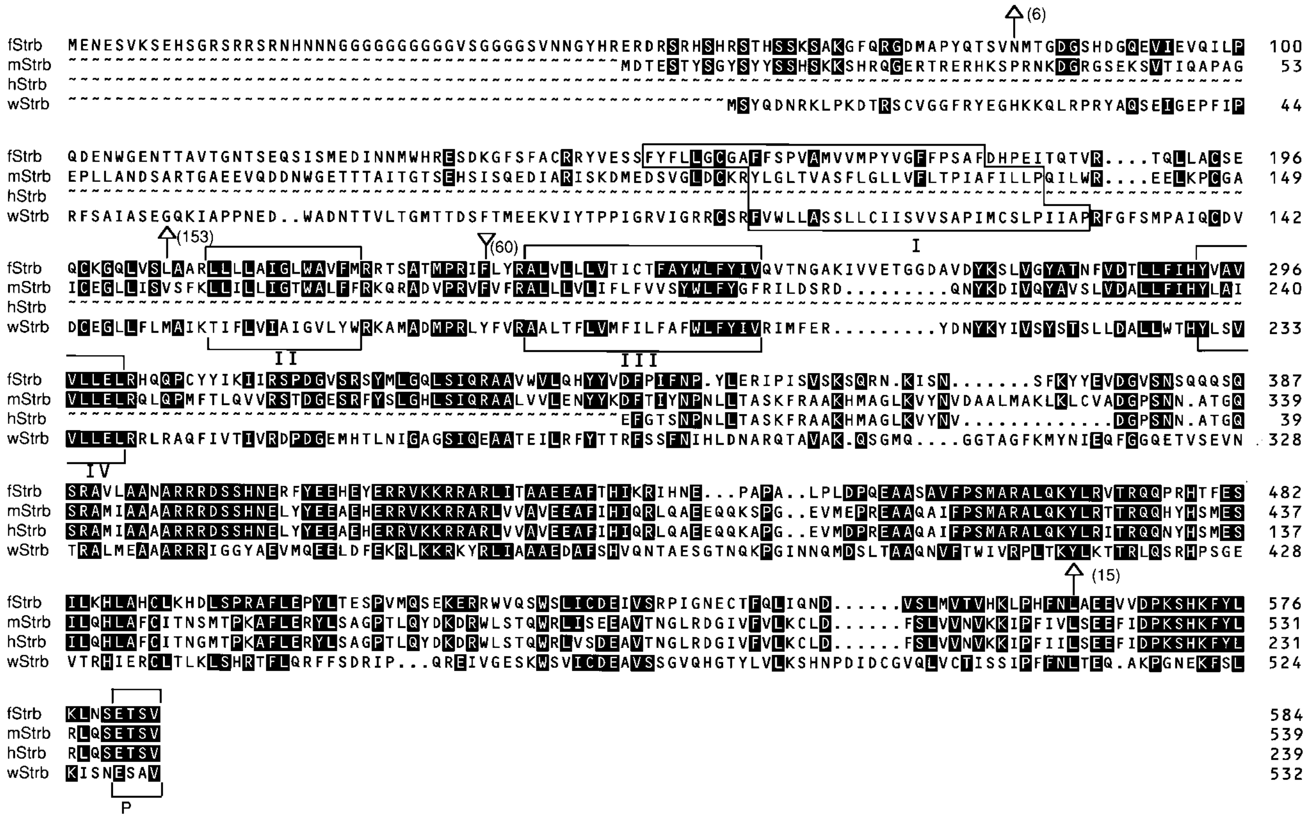

Fig. 7. The *stbm* coding region is not interrupted by introns. A 3.4 kb cDNA was sequenced and it contained a 162 bp 5′ UTR and a 1343 bp 3′ UTR. The predicted amino acid sequence of Stbm and its comparison to homologs from mouse, human and worm is shown. A conceptual translation of the open reading frame from the fly *stbm* cDNA is shown. The positions of mutations in four X-ray-induced *stbm* alleles are indicated (arrows); all alleles cause frame shifts in the ORF. Allele 6 is a 2 bp deletion at nucleotide 243 which creates a frame shift mutation at amino acid 81, thus truncating most of the protein. Allele 153 is a 7 bp deletion starting at nucleotide 614, causing a frame shift at amino acid 205. Allele 60 is a 4 bp duplication of adjacent sequence within codon 232. Allele 15 is a 5 bp deletion at nucleotide 1685 resulting in a frame shift 22 aa from the C terminus. Open reading frames for putative *stbm* genes from other species are also shown, and residues identical to *D. melanogaster* Stbm are highlighted. The mouse sequence was derived from a 3.7 kb cDNA and the human sequence is derived from a partial cDNA (accession no. T95333) which does not contain the entire ORF and is therefore not numbered. The worm sequence was identified by BLAST search (accession no. U52000) and eight putative exons were found to produce the sequence shown here. Domains I, II, III and IV were identified as hydrophobic regions using the Kyte-Doolittle algorithm (Kyte and Doolittle, 1982). Domains I and III are long enough to span the membrane and could serve to localize Stbm to the membrane. Although the amino acid sequences for domain I are not conserved, the hydrophobic nature of the region is conserved. Amino acid sequences for domains II, III, and IV are conserved between flies and the compared species. The P domain represents the putative PDZ domain-binding motif, which is identical between flies, mouse and humans, and in worms fits the consensus for this domain. This sequence has been deposited with GenBank under accession no. AF044208.

R4 cells can assume these fates in the absence of Stbm function (Fig. 2D), yet in these cases, the choice to become an R3 vs. an R4 cell appears to become randomized. This suggests that Stbm tips the balance such that the polar cell adopts the R4 fate, thus enabling chirality to be coordinated in the dorsal and ventral halves of the eye. In rare cases, R3 and R4 are symmetrical, possibly reflecting situations in which R3 and R4 remain undecided as to which fate to adopt.

Even though the R3 and R4 fates are often reversed in *stbm*⁻ ommatidia, the direction in which these mutant ommatidia rotate is usually consistent with the fates adopted by the R3 and R4 cells (the R3 fate is defined here as the cell that occupies the point of the trapezoid or has low H123 expression). In other words, in wild type, the equatorial cell always becomes an R3 and ommatidia always rotate such that the R1, R2 and R3 cells end up along the anterior side of the eye. When the R3 and R4 fates are reversed in the mutant, rotation subsequently becomes reversed such that R1, R2 and R3 still end up along the anterior face of the eye: in *stbm*⁻ clones, the large majority (81%) of genotypically mutant ommatidia rotate in a direction that is consistent with the identity of the R3 and R4 fates (46% normal orientation plus 35% D/V inversions). Therefore, rotation respects the identity of the R3/R4 cells in the majority of mutant ommatidia.

A minority of genotypically mutant ommatidia rotated ‘backwards’ with respect to the R3/R4 fates (7% A/P and 7% A/P and D/V inversions) and a few (5%) either failed to rotate or displayed rectangular trapezoids. These misrotated ommatidia can be explained as follows. The mosaic analysis shows that many, if not all, photoreceptors contribute to ommatidial orientation; for example, ommatidia in which only R1 is *stbm*⁻ can be misoriented. While these cells play a less important role than that of R3 and R4, their contribution is clearly not insignificant. Perhaps a ‘disagreement’ or

competition between R3/R4 and the remaining cell types leads to the delay in onset of ommatidial rotation in the eye disc.

An alternative possibility is that the ommatidia that are misrotated could represent ommatidia in which the future R3 and R4 cells were either undecided or switched fates following a key point when the rotation decision was made. A delay in the R3/R4 fate choice could also explain the delay in initiation of rotation in mutant eye discs.

The data from our analysis of mosaic ommatidia in which one cell of the R3/R4 pair is wild type and the other *stbm*$^{-}$ support the hypothesis that the direction an ommatidium rotates is largely determined by the fates of the equatorial and polar cells. As described above, ommatidia with the R3^{-}/R4^{+} genotype acquire an incorrect orientation in 74% of the cases. Furthermore, when both cells are mutant, their fates may be established randomly and thus their orientations more closely approximate a 50:50 distribution of phenotypically mutant and wild-type ommatidial forms.

We cannot rule out the possibility that *stbm* contributes directly to choosing the direction in which an ommatidium rotates. However, since ommatidia that rotate in a direction that is inconsistent with the R3/R4 cell fates are uncommon, it is likely that additional genes are needed for this decision.

While a detailed morphological analysis has not been conducted to define the order in which rotation and the specification of the R3/R4 occur, it is clear that the two events are virtually coincident. Our studies on *stbm* imply that the R3 and R4 fates are specified prior to activation of the 'rotation machinery'. One interpretation for the relationship between these two events is that the rotation machinery recognizes the R3/R4 fates and instructs the precluster to rotate in a direction consistent with this information (this has also been proposed by Zheng et al., 1995 and Choi et al., 1996). The mosaic analysis indicates that R3 and R4 are not the only photoreceptor precursors important for rotation; perhaps there are asymmetries in the other pairs of cells which can also provide supplementary information regarding the chirality of an ommatidium.

Comparison of *stbm* to other tissue polarity mutants

stbm mutant flies display many of the polarity phenotypes seen in *fz*, including ommatidial orientations in the eye, bristle and hair polarity in numerous epithelia, and duplications of leg segments. In addition, as in *stbm* mutants, the rotation of some ommatidia in *fz* eye discs is delayed (Zheng et al., 1995).

There are also a number of intriguing differences between the two genes. First, *fz* shows directional non-autonomy (it acts non-autonomously on the polar side of clones) (Vinson and Adler, 1987; Zheng et al., 1995) whereas *stbm* is ommatidium autonomous. This difference suggests that the two genes play distinct roles in the signaling pathway that sets up polarity. Second, the mosaic analyses of *stbm* and *fz* indicate that while *fz* is required to impart R3 identity on a cell, *stbm* is required for R4 cell identity. In *fz* ommatidia mosaic for the R3/R4 pair, the *fz*$^{+}$ cell adopts the R3 cell fate in 96% of cases (Zheng et al., 1995); a similar analysis of *stbm* showed that the *stbm*$^{+}$ cell adopted the R4 fate in 98% of all cases. A third significant difference is that *stbm* does not affect the center-lateral growth of new ommatidial rows whereas *fz* does. In their analysis of *fz*, Zheng et al. (1995) noted that preclusters at the ends of a leading row are often more mature than those close to the midline, suggesting *fz* mediates an equatorial signal for neuronal differentiation.

In addition to its similarity to the *fz* phenotype, *stbm* also bears a remarkable resemblance to tissue polarity phenotypes exhibited by *dsh* and *RhoA*, both in the eye and elsewhere. The similarity between the *stbm*, *dsh*, *fz* and *RhoA* phenotypes suggests that their gene products may function in the same or parallel pathways. In fact, genetic interactions have been demonstrated between *fz* and *dsh* (Krasnow et al., 1995; Strutt et al., 1997), *fz* and *RhoA*, and *RhoA* and *dsh* (Strutt et al., 1997).

Because of the phenotypic similarities between *stbm* and these other tissue polarity mutants, we have begun to look for genetic interactions between these genes. We were unable to identify obvious enhancement or suppression of the *stbm* phenotype by the removal of one copy of *pk*, *sple*, *fz*, *dsh* or *nmo* in a *stbm* mutant background. Furthermore, animals with mutations in both *stbm* and one of the above tissue polarity genes did not exhibit phenotypes that differed from those seen in *stbm* alone. The possible genetic and molecular relationship between these molecules and *stbm* will require further genetic and biochemical analysis.

Dfz2, a *Drosophila* Frizzled homologs, and Dsh have been implicated to act in the Wingless (Wg) signaling pathway. Dfz2 is the putative receptor for Wg (Bhanot et al., 1996), so the equatorial signal mediated by *fz* may be a Wnt. Dsh is required to transduce the Wg signal (see Klingensmith and Nusse, 1994 for review). Furthermore, Dsh contains a PDZ domain (Klingensmith et al., 1994; Theisen et al., 1994) and Stbm contains a PDZ domain-binding motif.

Conserved domains in the Stbm protein

Stbm shares no homology with known proteins, and with the exception of the putative PDZ domain-binding motif, there are no domains that suggest a possible role for Stbm. The existence of mammalian and worm homologs indicate the function of this protein is conserved. A structure-function analysis of this protein should help determine which regions are functionally important.

T. W. would like to express her gratitude to Marc Therrien and David Wassarman for their extensive expertise and patience in teaching her molecular biology; the cloning of *stbm* would not have been possible without their input. We are indebted to Todd Laverty for polytene chromosome analysis and Noah Solomon and Chris Suh for assistance with sequencing. We thank Bruce Hay for examining embryos and Kwang-Wook Choi and the Bloomington Stock Center for fly stocks. We are grateful to Mike Brodsky, Henry Chang, Ulrike Heberlein, Don Ready and David Wassarman for enlightening discussions and critical comments on the manuscript. We also thank John Tamkun for providing an aliquot of his cosmid library. T. W. is supported by an American Cancer Society fellowship and G. M. R. is a Howard Hughes Medical Institute Investigator.

REFERENCES

Altschul, S. F., Gish, W., Miller, W., Myers, E. W. and Lipman, D. J. (1990). Basic local alignment search tool. *J. Mol. Biol.* **215**, 403-410.

Bhanot, P., Brink, M., Samos, C. H., Hsieh, J.-C., Wang, Y., Macke, J. P., Andrew, D., Nathans, J. and Nusse, R. (1996). A new member of the *frizzled* family from *Drosophila* functions as a Wingless receptor. *Nature* **382**, 225-230.

Choi, K.-W. and Benzer, S. (1994). Rotation of photoreceptor clusters in the developing *Drosophila* eye requires the *nemo* gene. *Cell* **78**, 125-136.

Choi, K.-W., Mozer, B. and Benzer, S. (1996). Independent determination of symmetry and polarity in the *Drosophila* eye. *Proc. Natn. Acad. Sci. USA* **93**, 5737-5741.

Dietrich, W. (1909). Die facettenaugen der dipteren. *Z. Wiss. Zool.* **92**, 465-539.

Dougan, S. and DiNardo, S. (1992). *Drosophila* wingless generates cell type diversity among engrailed expressing cells. *Nature* **360**, 347-350.

Fanning, A. S. and Anderson, J. M. (1996). Protein-protein interactions: PDZ domain networks. *Curr. Biol.* **6**, 1385-1388.

Golic, K. G. and Lindquist, S. (1989). The FLP recombinase of yeast catalyzes site-specific recombination in the *Drosophila* genome. *Cell* **59**, 499-509.

Gubb, D. (1993). Genes controlling cellular polarity in *Drosophila*. *Dev. Suppl.* 269-277.

Hay, B. A., Wolff, T. and Rubin, G. M. (1994). Expression of baculovirus P35 prevents cell death in *Drosophila. Development* **120**, 2121-2129.

Held, L. I. Jr., Duarte, C. M., and Derakhshanian, K. (1986). Extra tarsal joints and abnormal cuticular polarities in various mutants of *Drosophila melanogaster*. *Roux's Arch. Dev. Biol.* **195**, 145-157.

Kimmel, B. E., Heberlein, U. and Rubin, G. M. (1990). The homeo domain protein rough is expressed in a subset of cells in the developing *Drosophila* eye where it can specify photoreceptor cell subtype. *Genes Dev.* **4,** 712-727.

Klingensmith, J., Nusse, R. and Perrimon, N. (1994). The *Drosophila* segment polarity gene *dishevelled* encodes a novel protein required for response to the *wingless* signal. *Genes Dev.* **8**, 118-130.

Klingensmith, J. and Nusse, R. (1994). Signaling by *wingless* in *Drosophila*.√ *Dev. Biol.* **166**, 396-414.

Krasnow, R. E., Wong, L. L. and Adler, P. N. (1995). *dishevelled* is a component of the *frizzled* signaling pathway in *Drosophila*. *Development* **121**, 4095-4102.

Kraut, R., Chia, W., Jan, L. Y., Jan, Y. N. and Knoblich, J. A. (1996). Role of *inscuteable* in orienting asymmetric cell divisions in *Drosophila*. *Nature* **383**, 50-55.

Kyte, J. and Doolittle, R. F. (1982). A simple method for displaying the hydropathic character of a protein. *J. Mol. Biol.* **157**, 105-132.

Lennon, G. G., Auffray, C., Polymeropoulos, M., and Soares, M. (1996). The I.M.A.G.E. consortium: an integrated molecular analysis of genomes and their expression. *Genomics* **33**, 151-152.

Melamed, J. and Trujillo-Cenoz, O. (1975). The fine structure of the eye imaginal disc in muscoid flies. *J. Ultrastruct. Res.* **51**, 79-93.

Ready, D. F., Hanson, T. E. and Benzer, S. (1976). Development of the *Drosophila* retina, a neurocrystalline lattice. *Dev. Biol.* **53**, 217-240.

Rhyu, M. S., Jan, L. Y. and Jan, Y. N. (1994). Asymmetric distribution of numb protein during division of the sensory organ precursor cell confers distinct fates to daughter cells *Cell* **76**, 477-491.

Robinow, S. and White, K. (1991). Characterization and spatial distribution of the ELAV protein during *Drosophila melanogaster* development. *J. Neurobiol.* **22**, 443-461.

Sambrook, J., Fritsch, E. F. and Maniatis, T. (1989). *Molecular Cloning: A Laboratory Manual*, Second Edition. Cold Spring Harbor, New York: Cold Spring Harbor Laboratory Press.

Sanger, F., Nicklen, S. and Coulson, A. (1977). DNA sequencing with chain terminating inhibitors. *Proc. Natl. Acad. Sci. USA* **74**, 5463-5467.

Songyang, Z., Fanning, A. S., Fu, C., Xu, J., Marfatia, S. M., Chishti, A. H., Crompton, A., Chan, A. C., Anderson, J. M. and Cantley, L. C. (1997). Recognition of unique carboxyl-terminal motifs by distinct PDZ domains. *Science* **275**, 73-77.

Strutt, D. I., Weber, U. and Mlodzik, M. (1997). The role of RhoA in tissue polarity and Frizzled signaling. *Nature* **387**, 292-295.

Tamkun, J. W., Deuring, R., Scott, M. P., Kissinger, M., Pattatucci, A. M., Kaufman, T. C. and Kennison, J. A. (1992). Brahma: a regulator of *Drosophila* homeotic genes structurally related to the yeast transcriptional activator SNF2/SWI2. *Cell* **XX**, 561-572.

Theisen, H., Purcell, J., Bennett, M., Kansagara, D., Syed, A. and Marsh, J. L. (1994). *dishevelled* is required during *wingless* signaling to establish both cell polarity and cell identity. *Development* **120**, 347-360.

Tomlinson, A. (1985). The cellular dynamics of pattern formation in the eye of *Drosophila*. *J. Embryol. Exp. Morph.* **89**, 313-331.

Tomlinson, A. and Ready, D. F. (1987). Cell fate in the *Drosophila* ommatidium. *Dev. Biol.* **123**, 264-275.

Vinson, C. R. and Adler, P. N. (1987). Directional non-cell autonomy and the transmission of polarity information by the *frizzled* gene of *Drosophila*. *Nature* **329**, 549-551.

Vinson, C. R., Conover, S. and Adler, P. N. (1989). A *Drosophila* polarity locus encodes a protein containing seven potential transmembrane domains. *Nature* **329**, 549-551.

Wolff, T. and Ready, D. F. (1991). The beginning of pattern formation in the *Drosophila* compound eye: The morphogenetic furrow and the second mitotic wave. *Development* **113**, 841-850.

Wolff, T. and Ready, D. F. (1993). Pattern formation in the *Drosophila* retina. In: *The Development of Drosophila melanogaster.* (ed. Michael Bate and Alfonso Martinez-Arias), pp. 1277-1325. Cold Spring Harbor, NY: Cold Spring Harbor Press.

Xu, T. and Rubin, G. M. (1993). Analysis of genetic mosaics in developing and adult *Drosophila* tissues**.** *Development* **117**, 1223-1237.

Zheng, L., Zhang, J. and Carthew, R. W. (1995). *frizzled* regulates mirror-symmetric pattern formation in the *Drosophila* eye. *Development* **121**, 3045-3055.